STABILITY ANALYSIS OF STATCOM

[1]Onah A. J., [2]Ezema E. E. and [3]Egwuatu I. D., and [4]Uzodife N. A.

[1]Michael Okpara University of Agriculture, Umudike, Nigeria. (aniagbosoonah@yahoo.com; 08030592574)

[2]Enugu State Polytechnic, Iwollo, Nigeria.

[3]Weiz Engineering, Ltd., Nigeria

[4] Department of Electrical Engineering, Federal Ministry of Works and Housing, Abuja, Nigeria.

Abstract One of the modern devices employed in reactive power compensation is the inverter-based static var compensator (SVC), otherwise known as STATCOM. The output voltage of the SVC is controlled by the angle between the inverter fundamental output voltage and the ac system voltage. A sensing and control system is required to monitor the ac system condition, and adjust this angle in order to supply reactive power to the system or absorb reactive power from the system, so as to regulate the bus voltage. The efficiency of a control system is usually measured by its stability. The aim of this paper is to show how stable the STATCOM can be when applied to a power system. The mathematical model of the STATCOM is derived, the system transfer function obtained and plotted. The stability of the system is then investigated, using the Routh's Tabulation, Bode diagrams, and root locus methods of stability analysis. Both the open-loop and closed-loop control systems were examined. The STATCOM was found to be stable for a wide range of values of the circuit parameters.

Index Terms— var compensation, STATCOM, stability, transfer function, Routh's tabulation, Bode diagrams, root locus.

1. Introduction

The STATCOM requires a good control strategy; application of a control system which incorporates power electronic-based controllers and other static controllers to improve controllability and power system operation flexibility, in order to optimize existing power systems [1]. Since the usefulness of every control system depends on stability, stability analysis of the STATCOM is carried out in this article. The control system measures and processes diverse parameters, like bus voltage, system frequency, and load of the system under compensation, determine the gating instants and issues the gating pulses to the solid-state switches in response to some system changes. The control system must, thus, be solidly synchronized to the ac system to avoid misfiring. For a control system to perform its function satisfactorily, it must be stable, meaning that it should respond creditably to input command, and it should not be sensitive to changes in system parameters [2]. In this paper the operational principle of the STATCOM is explained. The mathematical model is derived, the transfer functions obtained and used to analyze the stability of the system. In this work, we have applied some noted methods of stability analysis, such as the Routh;s tabulation, Bode diagrams, and root locus. It is also shown that the shortcoming of the open-loop control system can be offset by the closed-loop or feedback control. All the analysis methods show that the said STATCOM is stable and reliable control equipment.

1.1 Principle of Operation

The STATCOM achieves many goals such as system stability, provision of harmonic-free voltage at the

load bus, sinusoidal source current, load balance, and power factor correction [3]. Fig. 1 shows the circuit of a three-phase STATCOM topology. Its major component is a three-level, neutral point clamped (NPC), pulse width modulation (PWM) voltage source inverter (VSI) [4] It is connected to the ac mains through an inductor, X. The three-level inverter is more suitable than the two-level inverter in applications like static var compensation, traction systems, and flexible ac transmission systems, where high-voltage, high-power capability, and sinusoidal output voltage are needed [5]-[6].

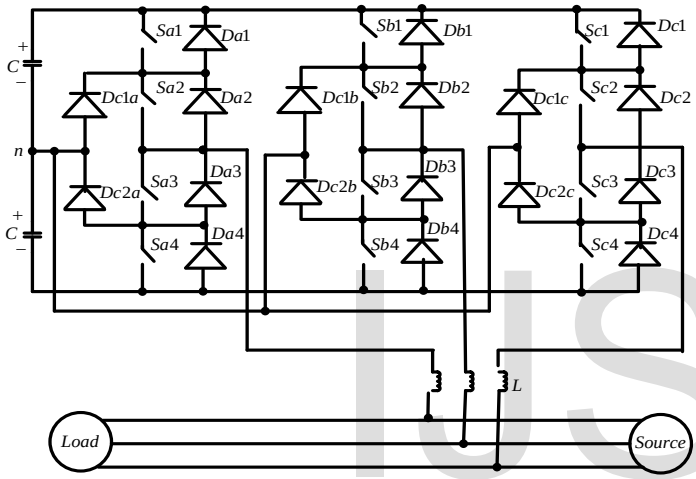

Fig. 1 Power Circuit of a STATCOM

The per-phase fundamental equivalent circuit of the STATCOM is shown in Fig. 2 and the phasor diagram is shown in Fig. 3.

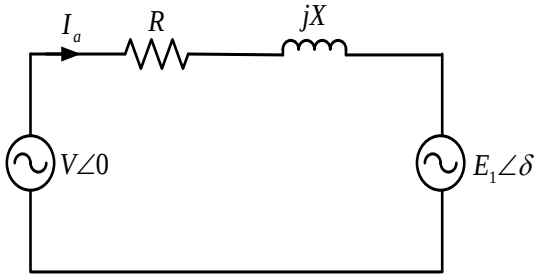

Fig. 2 Per-phase equivalent circuit of STATCOM at fundamental frequency

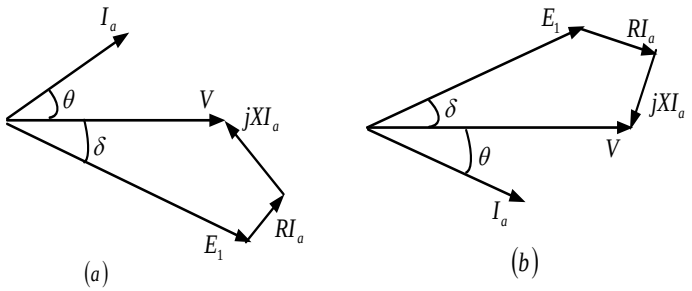

(a) Leading power factor

(b) Lagging power factor

Fig. 3 Phasor diagram

V = Line-to-neutral voltage of the ac mains.

E_1 = Fundamental component of the inverter phase-to-neutral ac voltage.

I_a = ac current

R = Losses of the system lumped

X= Line inductor

From Fig. 2, the apparent power supplied by the ac source can be expressed as

$$S = VI_a^* = |V|\angle 0\, I_a^* \quad (1)$$

$$I_a^* = \frac{|V|\angle 0 - |E_1|\angle -\delta}{R - jX} \quad (2)$$

$$S = \frac{|V|^2 - |V||E_1|\angle -\delta}{R - jX} \quad (3)$$

$$S = \frac{RV^2 - RVE\cos\delta - XVE\sin\delta}{R^2 + X^2} + \frac{jXV^2 + jRVE\sin\delta - jXVE\cos\delta}{R^2 + X^2}$$

Neglecting R

$$S = -\frac{VE\sin\delta}{X} + j\left(\frac{V^2 - VE\cos\delta}{X}\right) \quad (4)$$

Otherwise

$$S = \frac{1}{Z}\begin{bmatrix} V^2\cos\theta - VE\cos(\delta-\theta) \\ + j\left(V^2\sin\theta + VE\sin(\delta-\theta)\right) \end{bmatrix} \quad (5)$$

Where

$$Z = \sqrt{R^2 + X^2} \text{ and } \theta = \tan^{-1}\left(\frac{X}{R}\right)$$

δ = Phase-shift angle between the source voltage, V and the inverter ac voltage, E_1

The real power supplied by the ac source is shared by the load and the inverter. The amplitude of the fundamental component of the inverter output ac voltage, E_1 depends on the value of the dc bus voltage, V_{dc}. So, E_1 increases or decreases if the capacitor is charged or discharged. The voltage drop across X can be minimized by equalizing V and E, thus maintaining near unity power factor. The var compensator responds to fluctuations in load power factor by providing extra power required by the load or absorbing excess power from the load. If the power factor of the load increases, the load draws more real power which is transiently supplied by the compensator. The capacitor is thus discharged, leading to decrease in E_1. The control system takes corrective measure to make E_1 equal to the corresponding value of V and hence maintain the source power factor at near unity. This is done by making the phase-shift angle, δ negative and more active power will flow to the inverter to charge the capacitor. If the load power factor decreases, the load is taking less real power, and then the compensator absorbs the excess real power which charges the capacitor and then lead to higher output of E_1. To restore E_1 to normal value, the capacitor is discharged by giving δ a positive value. By controlling the phase angle δ, the dc capacitor voltage level can be changed, and thus the amplitude of the fundamental component of the inverter output voltage E_1 can be controlled [7]-[9]. Real power flows to the compensator if the load power factor is lagging (the load is drawing less active power); and the compensator supplies real power if load power factor is leading (load requires more active power). To reduce load power factor, the compensator has to absorb real power and supply reactive power ($\delta < 0$), and to raise load power factor, the compensator has supply real power and absorb reactive power ($\delta > 0$).

1.2 The Control Circuit:

The main circuit and control block diagram is shown in Fig. 4 [10]

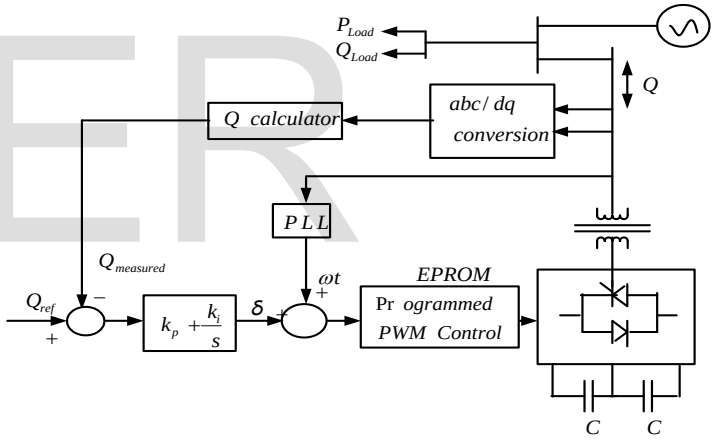

Fig.4 Main circuit and control block diagram.

As shown in Fig. 4, a phase locked loop (PLL) synchronizes the signal from a VCO with the ac supply, called the reference, so that they operate at the same frequency. The PLL synchronizes the VCO to the reference by comparing their phases (or frequency) and controlling the VCO so that its phase (or frequency) follows the changing reference phase (or frequency). The phase angle of the VCO is added to the control variable δ (output of the PI controller). This sum goes to the counter which addresses the EPROM where the programmed PWM switching pattern is stored. This PWM switching pattern enables the

elimination of selected number of harmonics, offers better voltage utilization, lower switching frequencies, less stress on switching devices and increased efficiency of the converter. The switching pattern is read at the supply frequency. The source voltage and current are transformed to d-q axis. The d-q quantities are used to calculate the reactive power generated by the system, and the calculated value is compared to the reactive power reference [11]-[12].

2. STATCOM Modeling

The STATCOM system shown in Fig. 1 is partitioned into several basic sub-circuits as shown in Fig. 5 [13]-[14] in order to simplify analysis. The sub-circuits are (A) voltage source, (B) resistor set, (C) inductor set, (D) switch set and (E) dc circuit.

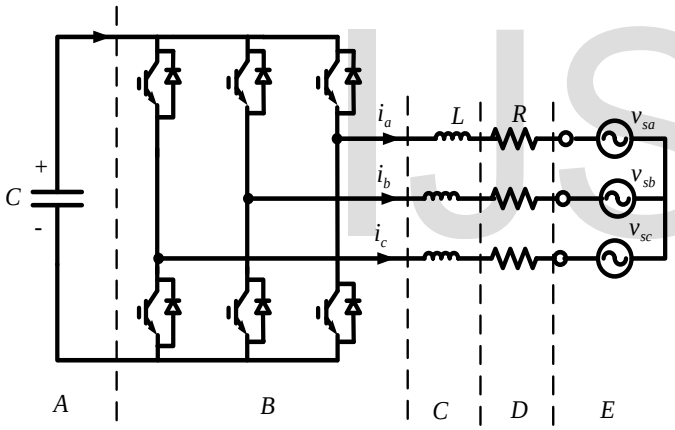

Fig. 5 Simplified main circuit of the ASVC system.

The mathematical model of the ASVC is obtained by transformation into the d-q reference frame, using the classic transformation matrix of equation (6) [15], and under the following assumptions [16]:

(i) All switches are ideal

(ii) Source voltages are balanced

(iii) Total loss of the inverter is represented by lumped resistor *R*

(iv) Harmonic components generated by switching action are negligible. Thus the switching functions are purely sinusoidal.

The power invariant d-q transformation matrix, *K* is given as:

$$K=\sqrt{\frac{2}{3}}\begin{bmatrix}\cos(\omega t) & \cos\left(\omega t-\frac{2\pi}{3}\right) & \cos\left(\omega t+\frac{2\pi}{3}\right)\\ \sin(\omega t) & \sin\left(\omega t-\frac{2\pi}{3}\right) & \sin\left(\omega t+\frac{2\pi}{3}\right)\\ \frac{1}{\sqrt{2}} & \frac{1}{\sqrt{2}} & \frac{1}{\sqrt{2}}\end{bmatrix} \quad (6)$$

The three-phase source voltag is:

$$v_{S,abc}=\begin{bmatrix}v_{sa}\\ v_{sb}\\ v_{sc}\end{bmatrix}=\sqrt{\frac{2}{3}}V_s\begin{bmatrix}\sin(\omega t+\delta)\\ \sin(\omega t-2\pi/3+\delta)\\ \sin(\omega t+2\pi/3+\delta)\end{bmatrix} \quad (7)$$

where V_s and ω denote the rms line-to-line voltage and the angular frequency of the source voltage respectively. The variable δ is the phase difference between the source voltage and the output voltage of inverter. The transformation is said to be power invariant by virtue of the coefficient $\sqrt{2/3}$ which makes the power calculated in *d-q* coordinate system the same as in the a*bc* system. The rotating three-phase circuits are now transformed to stationary circuits, eliminating the time-varying nature of the switching system. A variable f_{abc} that denotes any ac voltage or current is transformed into f_{qdo} by d-q transformation matrix *K*. That is:

$$f_{qdo}=Kf_{abc} \quad (8)$$

The relationship between voltage and current in the resistor *R* is:

$$v_{s,abc}=Ri_{abc}+v_{abc} \quad (9)$$

In d-q transform,

$$v_{s,qdo} = Ri_{qdo} + v_{qdo}$$

$$v_{s,qdo} = Kv_{s,abc}$$

$$v_{s,qd0} = V_s \begin{bmatrix} -\sin\delta \\ \cos\delta \\ 0 \end{bmatrix} \quad (10)$$

In the inductor, voltage and current relation is:

$$L\frac{di_{abc}}{dt} = v_{abc} - v_{o,abc} \quad (11)$$

$$KL\frac{di_{abc}}{dt} = Kv_{abc} - Kv_{o,abc} = v_{qdo} - v_{o,qdo} \quad (12)$$

It can be shown that

$$L\frac{di_q}{dt} = -\omega L i_d + v_q - v_{oq} \quad (13)$$

$$L\frac{di_d}{dt} = \omega L i_q + v_d - v_{od} \quad (14)$$

Since the harmonics generated by the switching action in the inverter are assumed negligible, the switching function, *S* is sinusoidal, and can be defined as:

$$S = \begin{bmatrix} S_a \\ S_b \\ S_c \end{bmatrix} = \sqrt{\frac{2}{3}} D \begin{bmatrix} \sin(\omega t) \\ \sin\left(\omega t - \frac{2\pi}{3}\right) \\ \sin\left(\omega t + \frac{2\pi}{3}\right) \end{bmatrix} \quad (15)$$

D is the r m s line-to-line amplitude of the switching function. With the switching function, the output voltage of the ASVC is obtained from the dc side capacitor voltage as follows.

$$v_{o,abc} = Sv_{dc}$$
$$v_{o,qdo} = Kv_{o,abc} = KSv_{dc} \quad (16)$$

$$v_{oq} = 0$$
$$v_{od} = Dv_{dc} \quad ; \quad (17)$$

$$i_{dc} = \frac{1}{2}S^T i_{abc} = \frac{1}{2}S^T K^{-1} i_{qdo} \quad (18)$$

$$2i_{dc} = Di_d \quad (19)$$

The switch set is exactly equivalent to the transformer whose turn ratio is defined to be the dual value of the duty cycle of the switch set [17]. These D-Q transformed sub-circuits are now connected together by joining adjacent ports that have the same variables as shown in Fig. 6, which is the equivalent circuit.

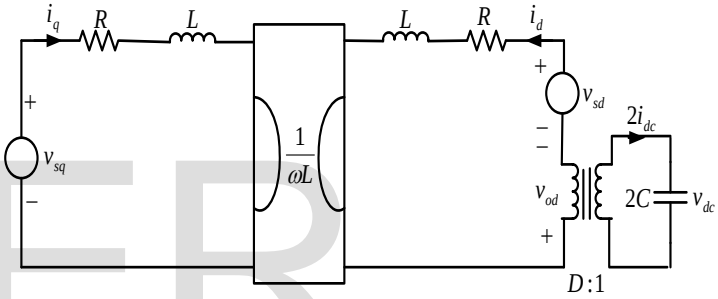

Fig. 6 Equivalent circuit of the ASVC

The following equations can be derived from the equivalent circuit:

$$v_{sq} = Ri_q + L\frac{di_q}{dt} + \omega L i_d \quad (20)$$

$$v_{sd} = Ri_d + L\frac{di_d}{dt} - \omega L i_q + V_{od} \quad (21)$$

$$Di_d = 2C\frac{dv_{dc}}{dt} \quad (22)$$

3. AC Analysis – phase angle (α) control

To see the dynamic characteristics of the STATCOM, the small signal equivalent circuit is derived by introducing some disturbances in the control variables around their operating points. The small

signal circuit is based on the following assumptions [18]:

(a) Harmonics are neglected as multi-pulse circuit configurations are employed to reduce generation of harmonics.

(b) The quiescent value of δ is small ($\left| \delta \right| < 5^{o}$)

(c) The disturbance, $\Delta\delta$ is nearly zero

(d) The second order terms (product of variables) are negligible.

$$\sin\delta \approx \delta ; \cos\delta \approx 1 \qquad (23)$$

Applying small perturbations to variables around their operating points and neglecting second order terms, we obtain the following results:

$$V_{od} = DV_{dc}$$

$$v_{od}(t) = V_{od} + \Delta v_{od} = (D + \Delta d)(V_{dc} + \Delta v_{dc})$$

$$\Delta v_{od} = D\Delta v_{dc} + \Delta d V_{dc} \qquad (24)$$

$$2I_{dc} = DI_{d}$$

$$2i_{dc}(t) = 2(I_{dc} + \Delta i_{dc}) = (D + \Delta d)(I_{d} + \Delta i_{d})$$

$$2\Delta i_{dc} \approx D\Delta i_{d} \qquad (25)$$

$$V_{sq} = -V_{s}\sin\delta$$

$$v_{sq}(t) = V_{sq} + \Delta v_{sq} = -V_{s}\sin(\delta + \Delta\delta)$$

$$\Delta v_{sq} = -V_{s}\Delta\delta \qquad (26)$$

$$V_{sd} = V_{s}\cos\delta$$

$$v_{sd}(t) = V_{sd} + \Delta v_{sd} = V_{s}\cos(\delta + \Delta\delta)$$

$$\Delta v_{sd} \approx 0 \qquad (27)$$

$$Q_{c} = V_{sq}I_{d} - V_{sd}I_{q} = -V_{sd}I_{q}$$

$$Q_{c} + \Delta Q_{c} = -V_{sd}(I_{q} + \Delta i_{q})$$

$$\Delta Q_{c} = -V_{sd}\Delta i_{q} = -V_{s}\cos\delta\,\Delta i_{q} = -V_{s}\Delta i_{q} \qquad (28)$$

Using equations (24), (25), (26) and (27) small signal equivalent circuit can be obtained from Fig. 6, as shown in Fig. 7

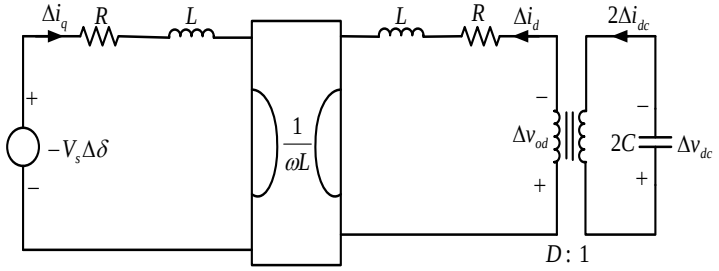

Fig. 7 Small signal equivalent circuit of the system

From the small signal equivalent circuit the following equations can be derived

$$L\frac{d\Delta i_{q}}{dt} = -R\Delta i_{q} - \omega L\Delta i_{d} - V_{s}\Delta\delta \qquad (29)$$

$$L\frac{d\Delta i_{d}}{dt} = -R\Delta i_{d} + \omega L\Delta i_{q} - D\Delta v_{dc} \qquad (30)$$

$$2C\frac{d\Delta v_{dc}}{dt} = D\Delta i_{d} \qquad (31)$$

A transfer matrix representation of the system is suitable for analysis and design [19]. So, equations (29), (30) and (31) in matrix form, give

$$\begin{bmatrix} \frac{d\Delta i_q}{dt} \\ \frac{d\Delta i_d}{dt} \\ \frac{d\Delta v_{dc}}{dt} \end{bmatrix} = \begin{bmatrix} -\frac{R}{L} & -\omega & 0 \\ \omega & -\frac{R}{L} & -\frac{D}{L} \\ 0 & \frac{D}{2C} & 0 \end{bmatrix} \begin{bmatrix} \Delta i_q \\ \Delta i_d \\ \Delta v_{dc} \end{bmatrix} + \begin{bmatrix} -\frac{V_s}{L} \\ 0 \\ 0 \end{bmatrix} \Delta\delta \quad (32)$$

The input of the system is the control variable, $\Delta\delta$ while the output is the generated reactive power, ΔQ

The state equation of the system is

$$\frac{dx}{dt} = Ax + B\Delta\delta \quad (33)$$

$$\Delta Q_c = Cx \quad (34)$$

$$x = \begin{bmatrix} \Delta i_q \\ \Delta i_d \\ \Delta v_{dc} \end{bmatrix}; \; A = \begin{bmatrix} -\frac{R}{L} & -\omega & 0 \\ \omega & -\frac{R}{L} & -\frac{D}{L} \\ 0 & \frac{D}{2C} & 0 \end{bmatrix}; \; B = \begin{bmatrix} -\frac{V_s}{L} \\ 0 \\ 0 \end{bmatrix};$$

$$C = \begin{bmatrix} -V_s & 0 & 0 \end{bmatrix}$$

Taking the Laplace transforms of equations (33) and (34):

$$sX(s) - X(0) = AX(s) + B\Delta\delta(s) \quad (35)$$

$$\Delta Q_c(s) = CX(s) \quad (36)$$

Equation (36) in (35) gives:

$$s\frac{\Delta Q_c(s)}{C} - X(0) = \frac{A\Delta Q_c(s)}{C} + B\Delta\delta(s) \quad (37)$$

$$\frac{\Delta Q_c(s)}{\Delta\delta(s)} = C(sI - A)^{-1}B \quad (38)$$

$$\frac{\Delta Q_c(s)}{\Delta\delta(s)} = \frac{\frac{V_s^2}{L}\left(s_2 + \frac{R}{L}s + \frac{D^2}{2LC}\right)}{s^3 + \frac{2R}{L}s^2 + \left(\frac{D^2}{2LC} + \left(\frac{R}{L}\right)^2 + \omega^2\right)s + \frac{D^2R}{2L^2C}} \quad (39)$$

Equation (39) is the open-loop transfer function of the system.

4. Open-loop Control

The Open-loop diagram is shown in Fig. 8

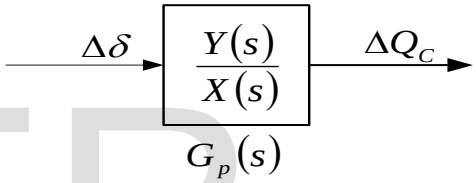

Fig. 8 Open-loop system

The following circuit parameters can be used to obtain the system transfer function:

Frequency, f = 50Hz

r-m-s line-to-line voltage, V_s = 400V

Resistance, R = 0.5Ω

Linked inductor, L = 27.4mH

DC side capacitor, C = 1000μF

Modulation index, $MI = \sqrt{\frac{2}{3}}\,D$ = 0.8

Phase angle, α = ±3

The transfer function becomes:

$$\frac{\Delta Q_c(s)}{\Delta\delta(s)} = \frac{5839s^2 + 106600s + 1.023x10^8}{s^3 + 36.5s^2 + 116500s + 319700} \quad (40)$$

In partial fraction, equation (40) is:

$$\frac{\Delta Q_c(s)}{\Delta\delta(s)} = \frac{2480.8 + j29.9}{s + 16.88 - j340.8} + \frac{2480.0 - j29.9}{s + 16.88 + j340.8} + \frac{877.3}{s + 2.75} \tag{41}$$

Equation (41) can be written as:

$$\frac{\Delta Q_c(s)}{\Delta\delta(s)} = \frac{4962\,(s + 16.88) - 59.8(340.8)}{(s + 16.88)^2 + (340.8)^2} + \frac{877.3}{s + 2.75} \tag{42}$$

The inverse Laplace transform gives:

$$g(t) = 4962\,e^{-16.88t}\cos 340.8t - 59.8e^{-16.88t}\sin 340.8t + 877.3e^{-2.75t} \tag{43}$$

The plot of equation (43) is shown in Fig. 9.

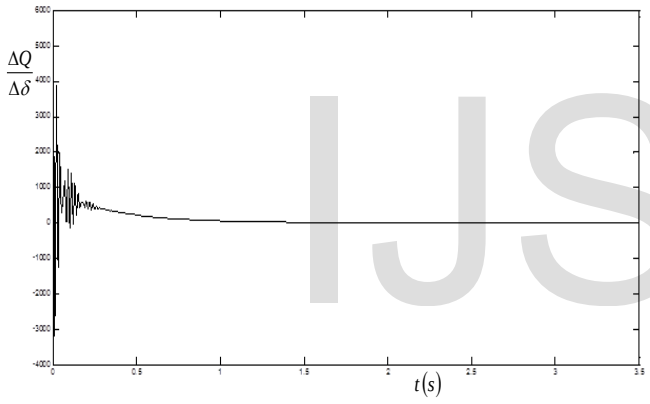

Fig. 9 Transfer function curve

It can be observed that equilibrium point is reached quickly in Fig. 9.

From equation (42)

$$\frac{\Delta Q_c}{\Delta\delta} = \frac{4962\,s + 63374}{s^2 + 33.76s + 116409} + \frac{877.3}{s + 2.75}$$

$$\frac{\Delta Q_c}{\Delta\delta} = \frac{14.56\omega_n s + 186\omega_n}{s^2 + 2\varepsilon\omega_n s + 285 + \omega_n^2} + \frac{319}{0.3636s + 1}$$

$$\frac{\Delta Q_c}{\Delta\delta} = \frac{0.043s + 0.546}{\left(\frac{s}{\omega_n}\right)^2 + 2\varepsilon\left(\frac{s}{\omega_n}\right) + 1} + \frac{319}{0.3636s + 1}$$

$$\frac{\Delta Q_c}{\Delta\delta} = \frac{0.546 + j0.043\omega}{\left(\frac{j\omega}{\omega_n}\right)^2 + 2\varepsilon\left(\frac{j\omega}{\omega_n}\right) + 1} + \frac{319}{j\omega T + 1} \tag{44}$$

Where

T = time constant = 0.3636s

ω_n = natural frequency of oscillation, 340.77 rads/s

ε = Damping ratio, 0.0495.

At low frequencies equation (42) can be approximated to a first order system given by:

$$\frac{\Delta Q_c}{\Delta\delta} = \frac{319}{j\omega T + 1} = \frac{A_o}{Ts + 1} \tag{45}$$

The step response of the system is given by:

$$\Delta Q_c(s) = \frac{-305.8s^2 - 5579s - 5356000}{s^4 + 36.5s^3 + 116500s^2 + 319700} \tag{46}$$

In partial fraction, equation (46) becomes:

$$\Delta Q_c(s) = \frac{0.0265 + j0.5151}{s + 16.88 - j340.8} + \frac{0.0265 - j0.5151}{s + 16.88 + j340.8} - \frac{16.8062}{s + 2.75} + \frac{16.7532}{s} \tag{47}$$

$$\Delta Q_c(s) = \frac{0.053\,(s + 16.88) - 1.03(340.8)}{(s + 16.88)^2 + (340.8)^2} - \frac{16.8062}{s + 2.75} + \frac{16.7532}{s} \tag{48}$$

The inverse Laplace transform gives:

$$\Delta q_c(t) = 0.053e^{-16.88t}\cos 340.8t - 1.03e^{-16.88t}\sin 340.8t - 16.8062e^{-2.75t} - 16.7532 \tag{49}$$

This is plotted as shown in Fig. 10

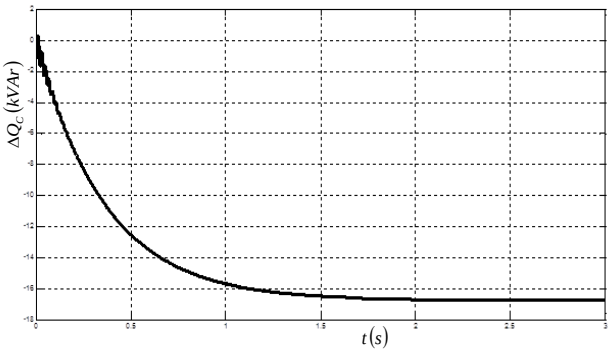

Fig. 10 Step response of the ASVC system.

From Fig 10, the system rise time = 0.792 s, settling time = 1.42 s, steady-state value = -16.8kVAr.

Under steady-state operation, the relation between the input and output quantities ($\Delta\delta$ and ΔQ) of the STATCOM can be shown to be:

$$Q_c = \frac{V_s^2}{2R}\sin 2\delta \qquad (50)$$

This is plotted as shown in Fig. 11.

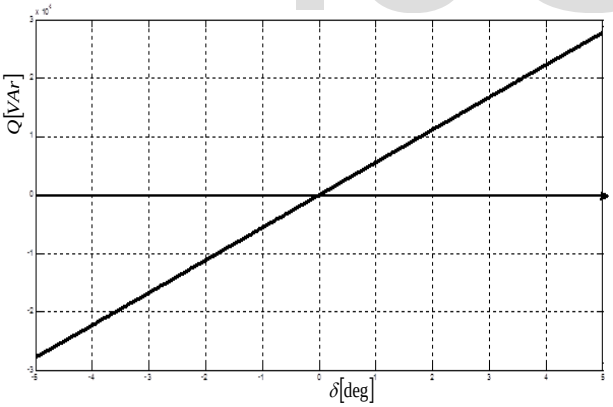

Fig. 11 Plot of the STATCOM output (Q) versus input (δ)

Both Fig. 10 and Fig. 11 show the sensitivity of the STATCOM to the input variable, δ

The stability of this system can be examined by the method of Routh's Tabulation as follows. The characteristic equation of the system is:

$$s^3 + 36.5s^2 + 116500s + 319700 \qquad (51)$$

s^3	1	116500
s^2	35.6	319700
s^1	107741	0
s^o	319700	0

$$\frac{(36.5)(116500)-(1)(319700)}{36.5} = 107741$$

$$\frac{(107741)(319700)-(36.5)(0)}{107741} = 319700$$

From the foregoing, all the elements of the first column of the Routh's Tabulation have the same sign, which means that all the roots of the characteristic equation are in the left half of the s-plane, and so the system is stable [2]. The roots are:

$-2.75, -16.88 + j340.8$ and $-16.88 - j340.8$

This system is a linear, single-input, single-output system. So, its response is completely dominated by the roots.

We can also investigate the stability of this system by means of the Bode diagram shown in Fig. 12

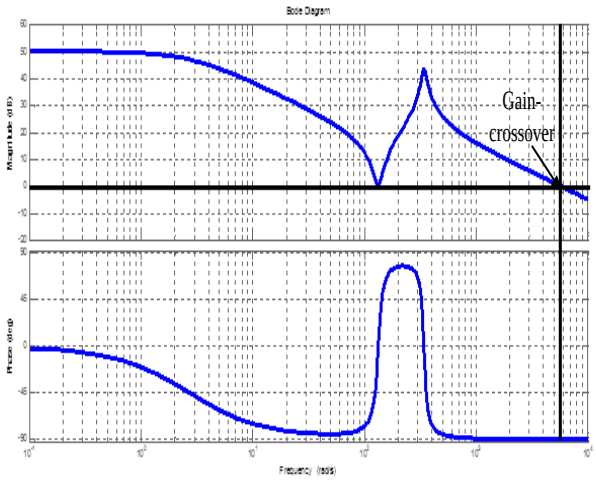

Fig. 12 Bode plot of system transfer function.

It can be observed from Fig. 12 that the:

Gain-crossover frequency =5860 rad/s.

Phase margin = -90^o-(-180^o) = 90^o

Phase-crossover is nonexistent, and so the Gain margin is infinity [19].

So, with the given parameters, the system is stable.

Now, we vary the value of each of the circuit components - capacitor, inductor, and resistor in equation (39), and see how they affect the stability of the STATCOM. The results are shown in the root loci of Fig. 13, Fig. 14 and Fig. 15. Fig. 13 is the root locus of the transfer function as the value of capacitance, C varies. It can be noticed that as C increases, the real negative root of the characteristic equation of the transfer function approach the imaginary axis. Roots nearer the imaginary axis have greater effect on the transient response of the system. This reduces the speed of the system response, and makes the system less stable. However, it can be noted that for this large range of C $\left(200 \le C \le 2000\mu F\right)$the roots are still in the left half of the s-plane, i.e. the system remains stable.

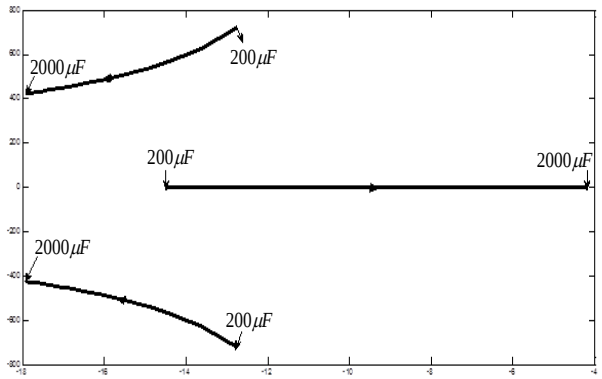

Fig. 13 Root locus for varying values of the dc Capacitor, C

The root locus of the system transfer function for increasing values of the inductance, L is shown in Fig. 14. The real negative roots as well as the complex-conjugate roots move towards the imaginary axis as the value of L increases. The compensator thus takes longer time to reach steady-state as L increases and consequently is less stable. However, it can be noted that for this large range of L $\left(5 \le L \le 100mH\right)$ the roots are still in the left half of the s-plane, i.e. the system is stable.

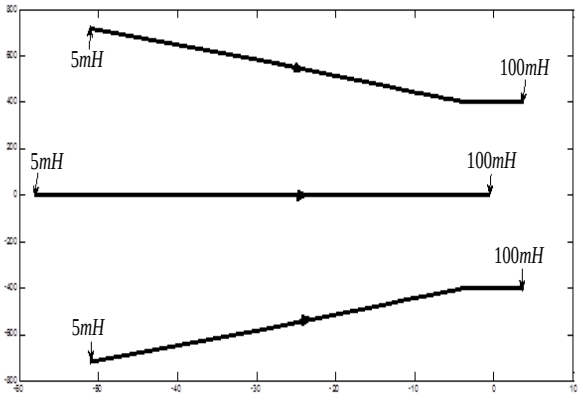

Fig. 14 Root locus for varying values of the line inductor, L

Fig. 15 is the root locus of the transfer function when the value of resistance, R varies. The real negative root as well as the complex-conjugate roots moves away from the imaginary axis as the value of R

increases. Thus, increasing the value of resistance, *R* speeds up the system response, enhancing stability. *R* is therefore a damping component.

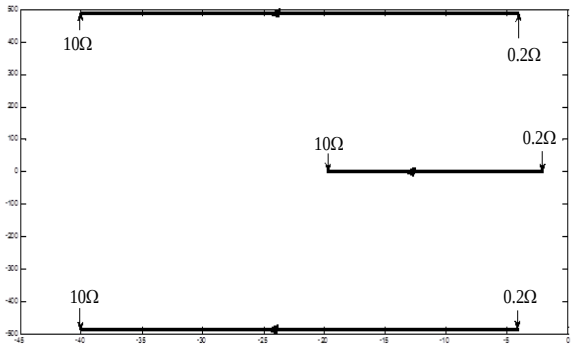

Fig. 15 Root locus for varying values of *R*

Generally, these figures show that the system is stable for a wide range of values of *C*, *L* and *R*. This is because all the roots remain in the left-half s-plane. So, it is obvious that varying the parameters of the STATCOM has little effect on the stability of the system.

5. Closed-loop Control

To realize a more accurate control, and stable system, feedback control can be employed. Here the controlled or output signal or a function of it is fed back to the controller, which compares it with the reference input signal. The difference between these signals is the error signal which has to be minimized in order to achieve the desired output. Fig. 16 is the closed-loop or feedback control system.

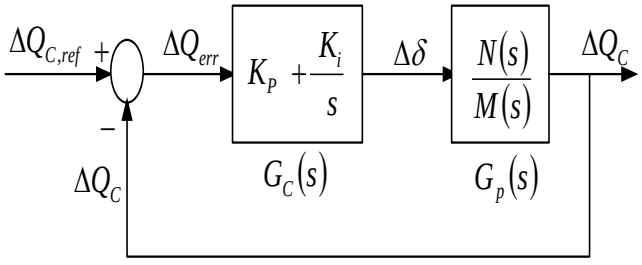

Fig. 16 Closed-loop block diagram of the STATCOM with PI controller

Thus from Fig. 16:

$$\left(\Delta Q_{C,ref} - \Delta Q_C\right)G_C(s)G_P(s) = \Delta Q_C \tag{52}$$

The closed-loop transfer function is given by:

$$\frac{\Delta Q_C}{\Delta Q_{C,ref}} = \frac{G_C(s)G_P(s)}{1+G_C(s)G_P(s)} \tag{53}$$

Equation (42) can be approximated to a first order system given by:

$$\frac{\Delta Q_c}{\Delta \delta} = \frac{877}{s+2.75} = G_P(s) \tag{54}$$

Step response of the first order system is shown in Fig. 17. It has the same characteristics as the third order system of Fig. 10.

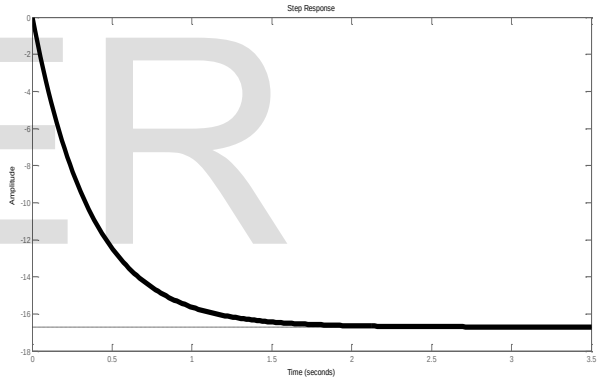

Fig. 17 Step response of the first order system

Equation (54) in (53) gives:

$$\frac{\Delta Q_C}{\Delta Q_{C,ref}} = \frac{877\left(K_p s + K_i\right)}{s^2 + \left(2.75 + 877K_p\right)s + 877K_i} \tag{55}$$

Fig. 18 shows the step response of the closed-loop control system.

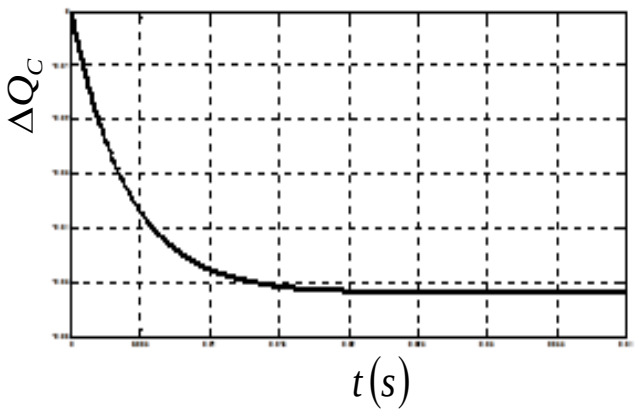

Fig. 18 Step response of closed-loop control system

From Fig. 18: rise time = 0.00923s, settling time = 0.0185s, peak amplitude = -0.0518 p.u.

Comparing the transfer function and the response obtained with the closed-loop system to those of the open-loop system shows that the closed-loop control system gives better stability and more accurate control.

Fig. 19 is the op-amp model of the PI controller

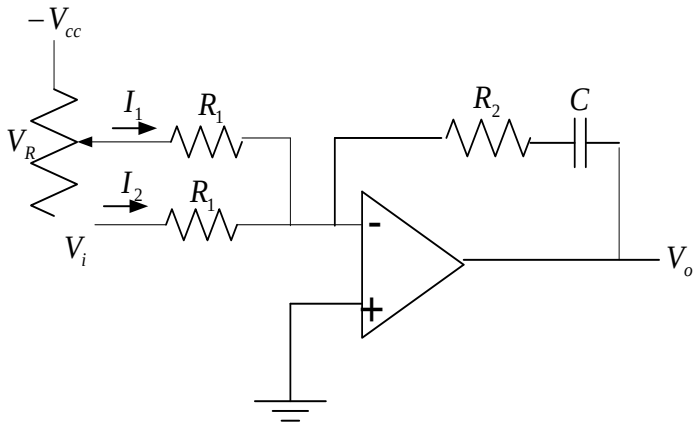

Fig. 19 Op-amp circuit realization of the PI controller

The transfer function of the op-amp circuit can be derived as:

$$K_p(V_R - V_i) + K_i\left(\int_0^t (V_R - V_i)dt\right) \quad (56)$$

$$-V_R + V_i = (i_1 + i_2)R_1 \quad (57)$$

$$V_o = -(i_1 + i_2)R_2 - \frac{1}{C}\int (i_1 + i_2)dt \quad (58)$$

$$V_o = (V_R - V_i)\left[\frac{R_2}{R_1} + \frac{1}{R_1 Cs}\right] \quad (59)$$

$$V_o = (V_R - V_i)\left[K_p + \frac{K_i}{s}\right] \quad (60)$$

$$\frac{V_o}{(V_R - V_i)} = \left[K_p + \frac{K_i}{s}\right] \quad (61)$$

6. Conclusion

The features and operational principles of a static var compensator (SVC) employing PWM voltage source inverter with self-controlled dc bus, otherwise known as STATCOM have been discussed in this paper. A model was derived, using d-q reference axis, for a var compensator operating with the δ phase-shift angle control. The model has been used to investigate the speed of response of the STATCOM to changing conditions and the stability of the compensator in relation to its circuit parameters. Results show that the compensator under discussion is stable for wide variations of its circuit parameters. It is shown also that, with smaller circuit parameters, the compensator reaches steady-state faster and is therefore more stable. The closed-loop system provides more stable and efficient control strategy than the open-loop control system.

References

[1] Rahul, D., Subhransu R.S., Bijay, K.P. and Vijendran, G.V. (2016). Exreme Learning Machine Based Adaptive Distance Relaying Scheme for Static Synchronous Series Compensator Based

Transmission Lines. Electric Power Components and Systems, 44(2), pp. 219-232.

[2] Benjamin C. K. and Golnaraghi, F. (2003). Automatic Control Systems. 8. Ed. New York: John Wiley & Sons Inc., p. 6-395

[3] Santos, R. N., Edison R. C., Cursino, B. J., Eisenhawer M. F., Alexandre C. O., Rafael R. M., Dalton F. G., Otacilio M. A. and Patryckson M. S. (2014). The Transformerless Single-phase Universal Active Power Filter for harmonic and Reactive Power Compensation. IEEE Transactions on Power Electronics, 29 (7), pp. 3563-3572.

[4] Wei C., Haiwei S., Xin G. and Changliang X. (2016). Synchronized Space-vector PWM for Three-Level VSI with Lower Harmonic Distortion and Switching Frequency. IEEE Transactions on Power Electronics, 31(9), pp. 6428 – 6441.

[5] Roozbeh N., Arash K. S. and Keyue M. S. (2016). Dual Flying Capacitor Active-Neutral-Point-Clamped Multilevel Converter. IEEE Transactions on Power Electronics, 31(9) pp. 6476-6484

[6] Yang J., Sizhao L. and Fred C. L. (2014). Switching Performance Optimization of a High Power High Frequency Three-Level Active Neutral Point Clamped Phase Leg. IEEE Transactions on Power Electronics, 29(7), pp. 3255-3266.

[7] Lasseter, R. H. and Ronghai W. (1999). The Impact of Generation mix on Placement of Static Var Compensators. IEEE Transactions on Power Delivery, 14(3).

[8] Fujita, H., Shinji T. and Hirofumi A. (1996). Analysis and Design of a DC Voltage-Controlled Static Var Compensator Using Quad-Series Voltage-Source Inverters. IEEE Transactions on Industry Applications, 32(4), pp. 482-488

[9] Trainer, D.R., Tennakoon S.B. and Morrison, R.E. (1994). Analysis of GTO-based static Var Compensator. IEE Proc.-Electr. Power Appl., 141(6), pp. 293-302.

[10] Benghanem, M. and Draou, A. (2006). A new Modelling and Control Analysis of an Advanced Static Var Compensator using a Three-level (NPC) Inverter Topology. Journal of Electrical Engineering, 57(5), pp. 285-290.

[11] Joos, G., Luis M. and Phoivos Z. (1991). Performance Analysis of a PWM Inverter Var Compensator. IEEE Transactions on Power Electronics, 6(3). pp. 380 – 390.

[12] Draou, A., Benghanem, M. and Tahri, A. (2000). Control and Dynamic Analysis of a Static Var Compensator using a Three-level Inverter Topology. 12th International Conference on Micrelectronics, Tehran, Oct. 31-Nov. 2, pp. 353-356, 2000.

[13] Guk C. C., Chun T. R., Nam S. C. and Gyu H. C. (2008). Modeling, Analysis and Control of Static Var Compensator Using Three-level Inverter. IEEE Transactions on Power Delivery, 11(1), pp. 837-843.

[14] Ramirez D., Martinez S., Blazquez F., Carrero C. (2012). Use of STATCOM in wind farms with fixed-speed generators for grid code compliance. Renew Energy 37(1), 202–212.

[15] Farhad S., Sumedha, R. and Arindam G. (2015). Static Compensators (STATCOMs) in Power Systems. Springer Singapore.

[16] Cho, G. C., Jung, G. H., Choi, N. S. and Gyu, H. C. (1996). Analysis and Controller Design of Static Var Compensator Using Three- level GTO Inverter. IEEE Transactions on Power Electronics, 11, pp. 57-65.

[17] Rim, C. T., Dong Y. H. and Gyu H. C. (1990). Transformers as Equivalent Circuits for Switches: General Proofs and D – Q Transformation-Based Analyses. IEEE Transactions on Industry Applications, 26(4), pp. 777-784.

[18] Carlos E. U., Eduardo L. C., Enrique A., Liceaga C. (2008). Fundamental Analysis of the Static Var Compensator Performance Using Individual Channel Analysis and Design. International Journal of Emerging Electric Power Systems, 9(2), pp. 1-32.

[19] Ogata, K. (2002). Modern Control Engineering.
4. ed. Delhi: Pearson Education, Inc., p. 497-523